Supporting information of

Albumin-Based Near-Infrared Phototheranostics for Frequency Upconversion Luminescence/ Photoacoustic Dual-Modal Imaging-Guided Photothermal Therapy

Hui Yu,[a] Aliya Tiemuer,[a] Yanyan Zhu,[a] Ye Sun,[a] Yuanyuan Zhang,[a] Li Liu*[c], Yi Liu * [a,b]

[a] Department of Biomedical Engineering, School of Engineering, China Pharmaceutical University, Nanjing, 211198, China.

[b] Jiangsu Key Laboratory for Biosensors, Institute of Advanced Materials (IAM), Nanjing University of Posts & Telecommunications, 9 Wenyuan Road, Nanjing 210023, China.

[c] Clinical Laboratory, Xiantao First People's Hospital, Xiantao, 433000, China.

* Corresponding author. E-mail addresses: yiliu@cpu.edu.cn (Y. Liu), liuli97892022@163.com (L. Liu).

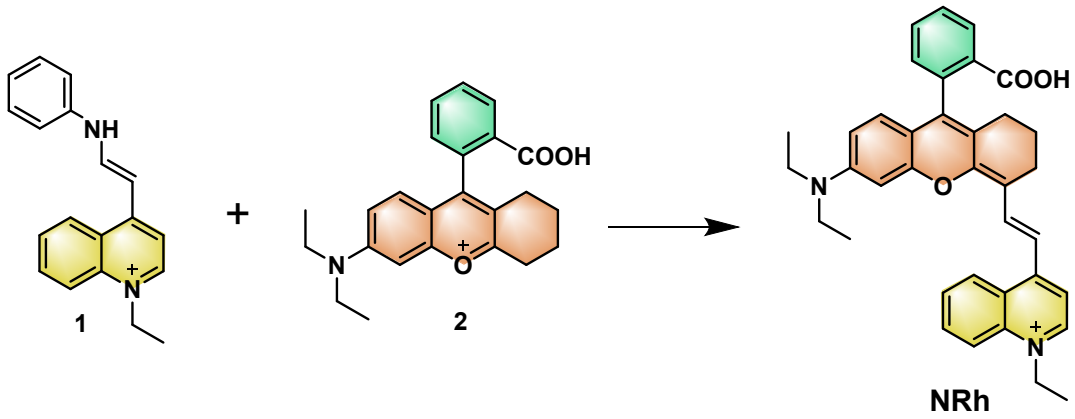

Scheme S1. Chemical structure and synthetic route of **NRh**.

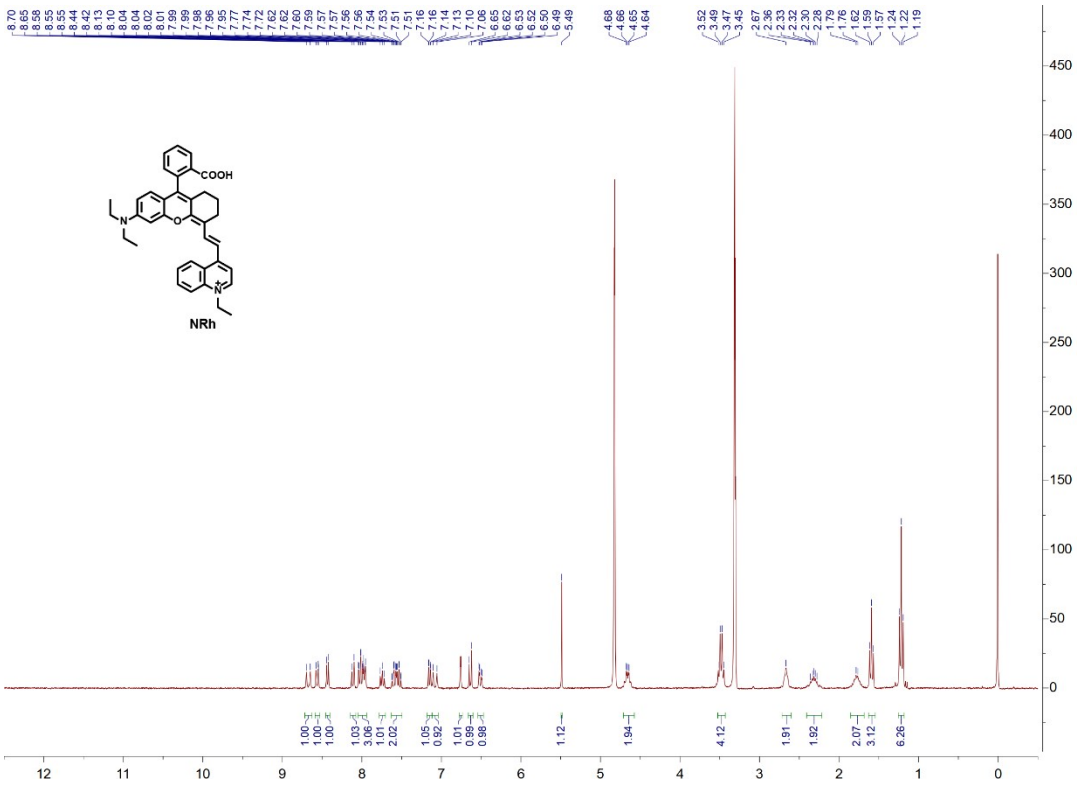

Fig. S1 The ^{1}H NMR spectrum of compound **NRh**.

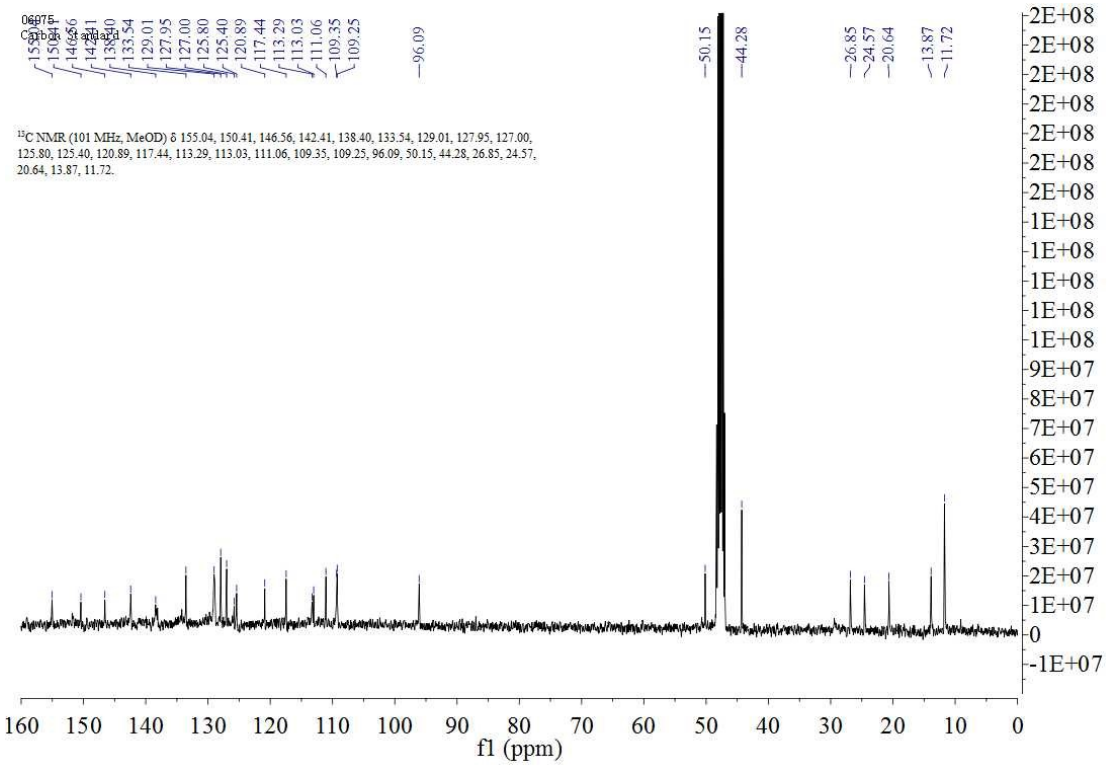

Fig. S2 The ^{13}C NMR spectrum of compound **NRh**.

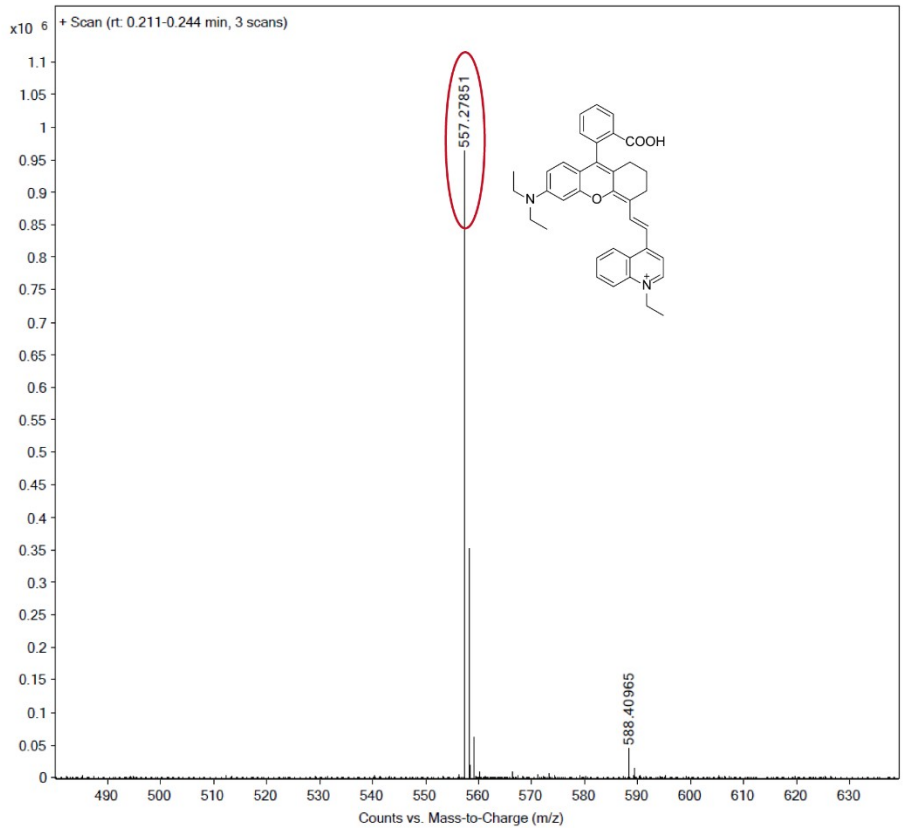

Fig. S3 High-resolution mass spectra of compound **NRh**.

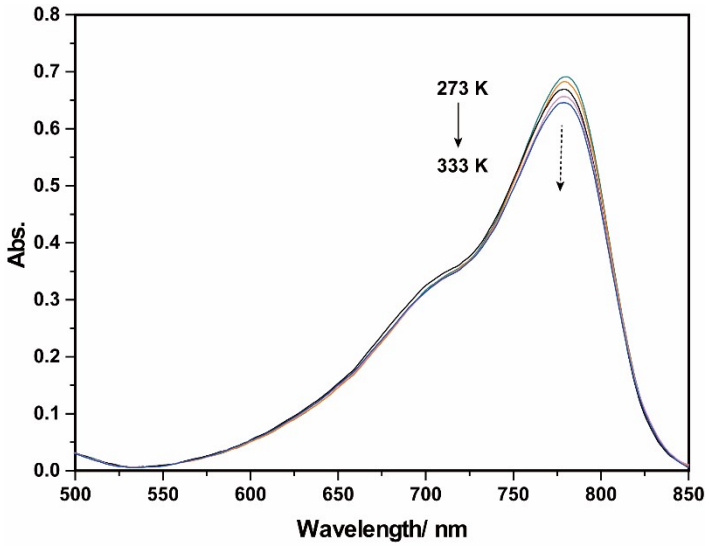

Fig. S4 Absorption spectra NRh in ethanol at different temperatures.

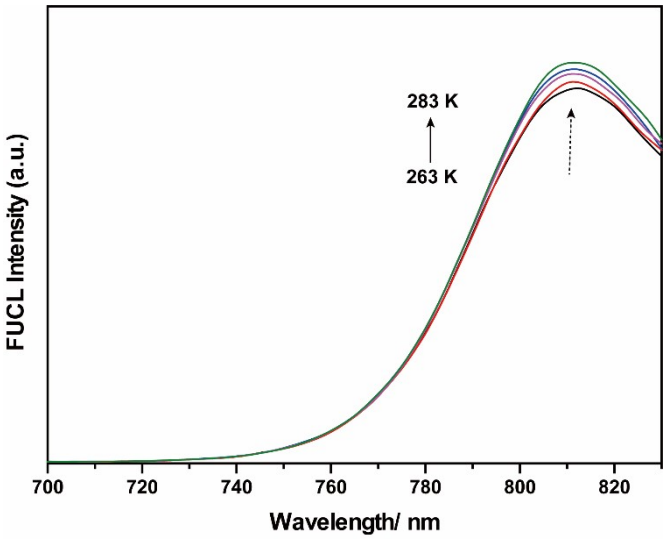

Fig. S5 FUCL emission spectra of NRh in ethanol at different temperatures.

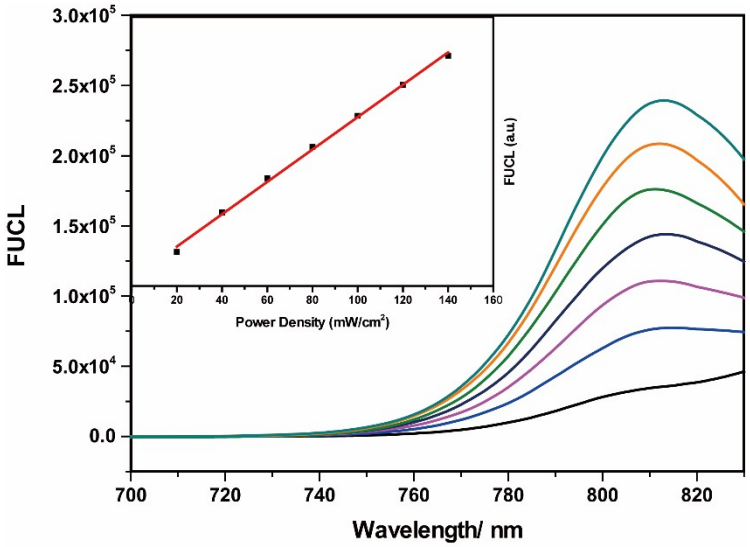

Fig. S6 FUCL emission spectra of NRh in ethanol at different power density. (Insert: FUCL emission intensity as a function of power density (Ex = 850 nm).

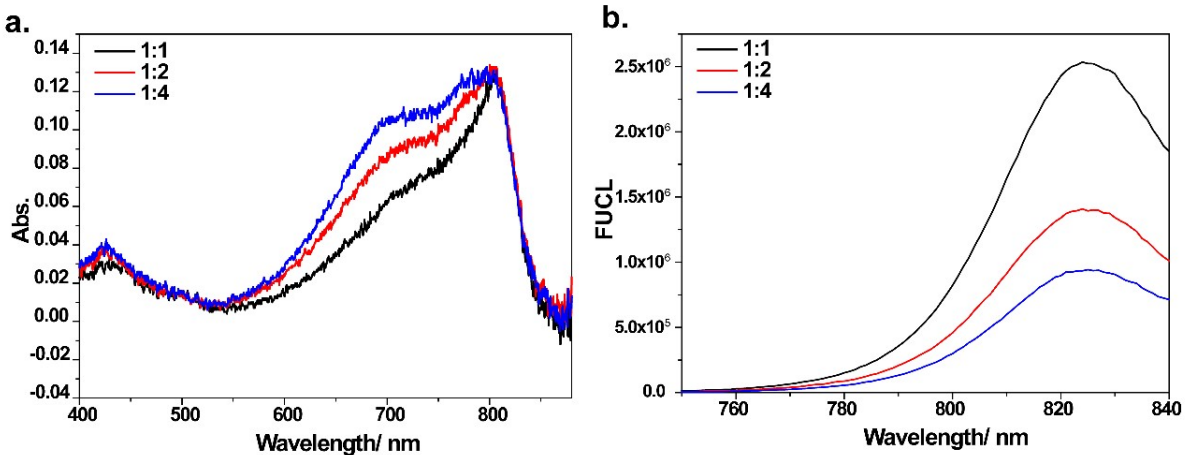

Fig. S7 Absorption spectra and FUCL emission spectra of NRh-BSA NPs with different molar ratios of NRh and BSA (1:1, 1:2 and 1:4).

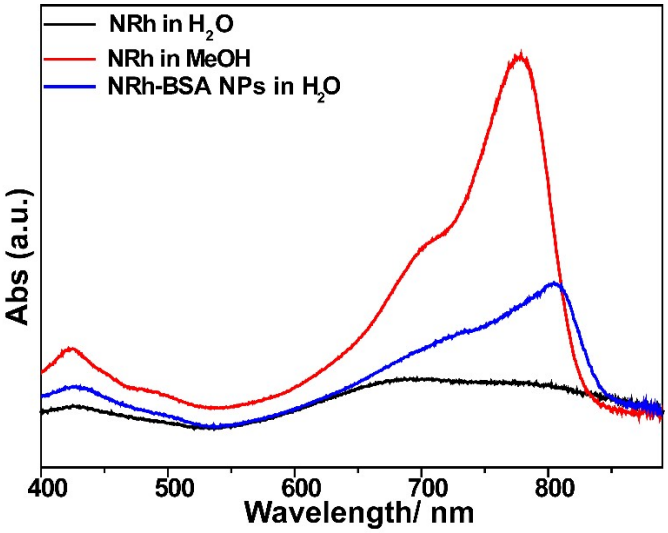

Fig. S8 Absorption spectra of NRh, NRh-BSA NPs in H_2O and NRh in MeOH.

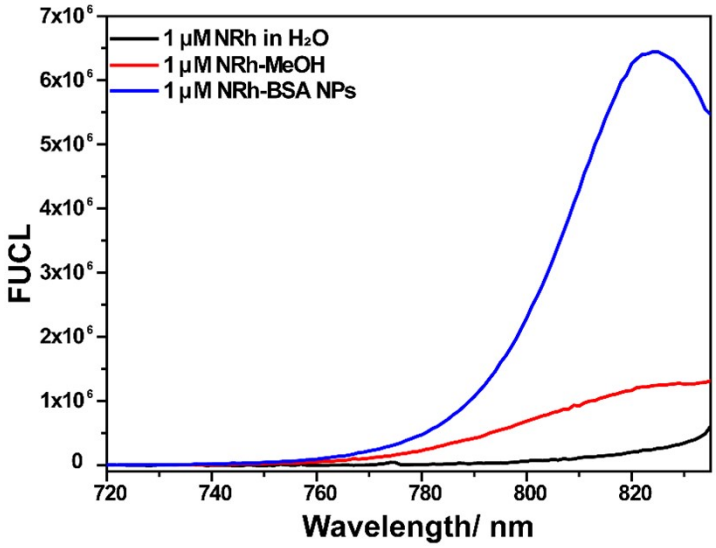

Fig. S9 FUCL emission spectra of NRh, NRh-BSA NPs in H_2O and NRh in MeOH.

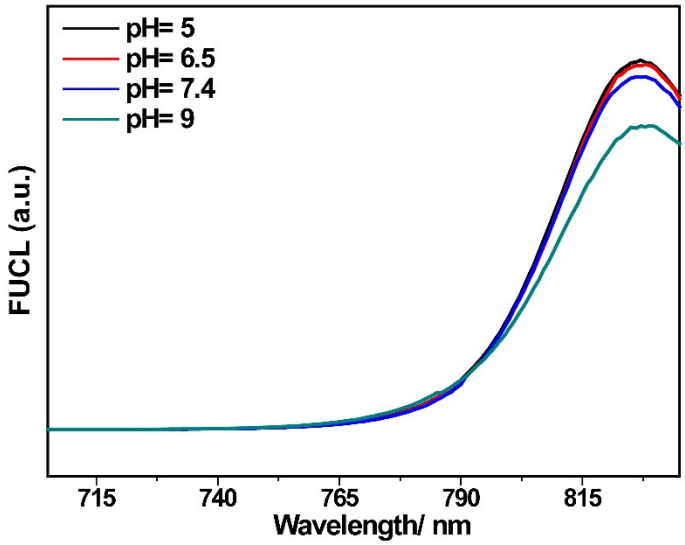

Fig. S10 FUCL emission spectra of NRh-BSA NPs at different pH.

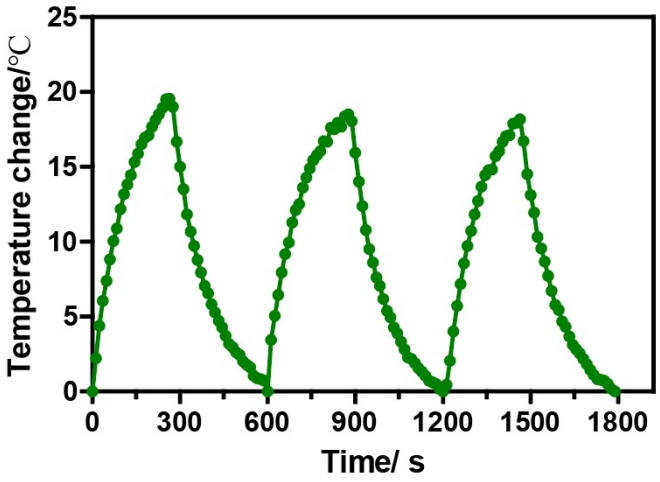

Fig. S11 Heating and cooling curves of NRh-BSA NPs for three cycles by turning on and off laser.

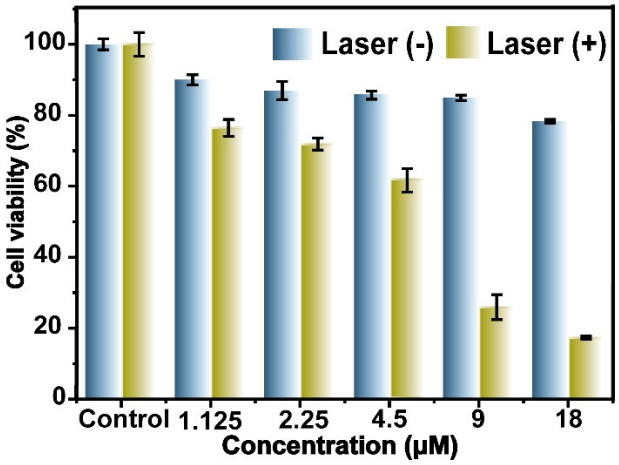

Fig. S12 Cell viabilities of U87MG cells incubated with NRh-BSA NPs at various concentrations.

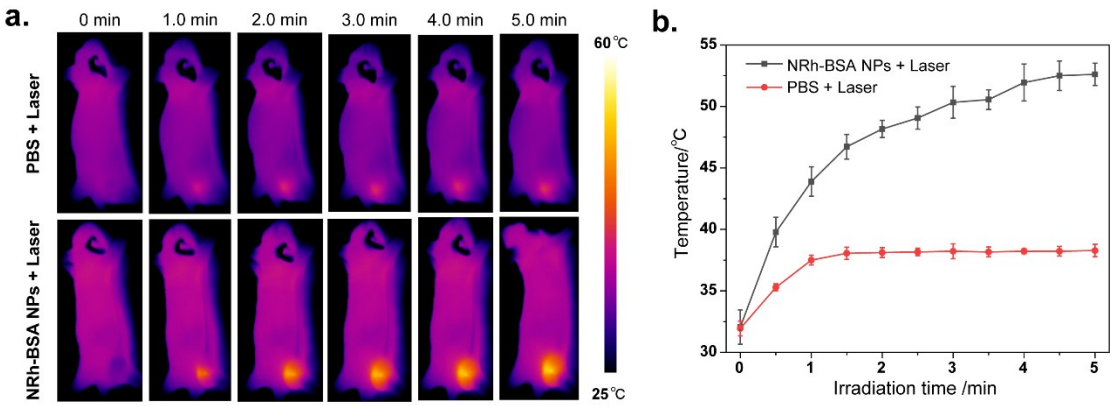

Fig. S13 Thermographic images and corresponding temperature increase of U87 MG tumor-bearing mice exposed to 808 nm laser (1 W/cm^2) for 5 min with or without injection of NRh-BSA NPs.